SLAC–PUB–5725
June 1992
(A/I)

A SIMPLE MODEL FOR SLC POSITRON STABILITY ISSUES *

P. Krejcik and V. Ziemann

Stanford Linear Accelerator Center,

Stanford University, Stanford, CA 94309

ABSTRACT

A simple model is constructed for the SLC positron system to describe the intensity variations induced by beam loading in the linac. It is found that the system can be described by the well known logistic equation. This allows us to use results from the stability analysis to characterize the positron system, to place tolerances on fluctuations, and to slow variations on the scavenger beam intensity.

Presented at the General Meeting of the American Physical Society,

Washington, DC, April 20–23, 1992

*Work supported by Department of Energy contract DE–AC03–76SF00515.

I. INTRODUCTION

A design feature of the SLC is that the positron bunch, the electron bunch, and the second electron bunch (usually called scavenger bunch), share a common high-energy linac structure. This causes the bunches to interact via beam loading. The leading bunch in this train is the positron bunch, so its intensity affects the energy of the following electron bunch and scavenger bunch, that is used to produce the positrons for the next pulse. Its energy variation leads to particle losses in the extraction line and affects the positron bunch intensity on the next pulse. This establishes an iterative mechanism in which the positron intensity depends on the intensity of the previous positron bunch.

The strongest part of the bunch-to-bunch interaction comes from the finite energy aperture of the Sector 19 scavenger electron extraction line. The energy acceptance of the extraction line is on the order of a few percent. The energy of the scavenger electrons can easily change by this amount as a result of beam loading in the linac at typical SLC intensities. Since fluctuations in the scavenger energy—either up or down—both lower the positron intensity, our simple model uses a quadratic dependence.

When the positron bunch intensity at the target changes, there are additional effects in the downstream positron system that further amplify these intensity changes. They may also modify the quadratic dependence by making it asymmetric and of higher order.

In this simple model, we lump all these effects into the quadratic function and analyze its implications.

II. A SIMPLE MODEL

In this model we denote the number of positrons at Sector 19 that were produced without the above mentioned feedback mechanism by

$$p_0 = \eta s_0 \,. \tag{1}$$

Here s_0 is the intensity of the scavenger bunch at the gun, assumed to be produced continuously, and η is the product of the efficiencies through the individual subsystems. Therefore, p_0 is the number of positrons in Sector 19 if the gun continuously produced s_0, the product of efficiencies were η, and there were no effect of beam loading. However, one of those efficiencies describes the number of positrons in the positron return line as a function of the number of scavenger electrons in Sector 19. The effect of beam loading on this efficiency can now be incorporated into the model by multiplying η by

$$1 - \alpha_- \left(\frac{e_{n-1} - \hat{e}}{\hat{e}} \right)^2 - \alpha_+ \left(\frac{p_{n-1} - \hat{p}}{\hat{p}} \right)^2 ,$$

where the subscript n refers to the pulse number. In 120 Hz operation, pulses are separated by 8.3 ms. Here p_{n-1} denotes the positron intensity at Sector 19 on the $n-1^{th}$ pulse, and $\hat{e}$ and $\hat{p}$ are the design electron and positron currents for which beam loading is compensated. They are usually adjusted by klystron phases in Sectors 17 and 18. α_- and α_+ are coefficients that describe the strength of the feedback mechanism. The magnitude of the α is addressed below.

In this model, the degrading effect of the beam loading on positron intensity is described by a quadratic function that simply addresses the fact that an off-energy scavenger bunch reduces the number of positrons, no matter whether the energy

is too high or too low. Later this can be developed into a more sophisticated model to include additional effects, such as noise induced by fluctuations in the electron intensity or a modification of the quadratic dependence on the previous pulse.

In what follows, we will always assume that the electron intensity is constant and always properly compensated [$e(n) = \hat{e}$]. The equation that determines the dynamics of this model can thus be written

$$p_n = \eta s_0 \left[1 - \alpha_+ \left(\frac{p_{n-1} - \hat{p}}{\hat{p}} \right)^2 \right] . \tag{2}$$

The magnitude of α_+ can be estimated as follow. In the Blue SLC Design Handbook (pp. 2–28), the energy loss of a following bunch is estimated to be 890 MeV per 5×10^{10} particles at Sector 30. We can convert this number into an energy loss of the scavenger bunch at Sector 19, and write

$$\frac{d\,E_{\rm scav}(n)}{d\,p_{n-1}} = \frac{19}{30} \frac{890\,{\rm MeV}}{5 \times 10^{10}} \approx \frac{100\,{\rm MeV}}{10^{10}} . \tag{3}$$

A $\Delta p/p = 1\%$ positron intensity variation thus translates into a 1 MeV energy offset of the scavenger bunch, which translates into a relative energy offset of

$$\frac{\Delta E}{E} = \frac{1\,{\rm MeV}}{30\,{\rm GeV}} = 3.3 \times 10^{-5} . \tag{4}$$

The present extraction line collimators are configured such that a 1% energy offset reduces the positron yield by 50%. Therefore, a 1% positron intensity variation of the previous bunch changes the next positron intensity by

$$r(1\%) = \frac{50\%}{1\%}\ 3.3 \times 10^{-5} . \tag{5}$$

where $r(1\%)$ is the fractional yield reduction of a scavenger bunch due to a 1% intensity variation in the previous positron bunch. We can calculate α_+ from

$$1 - \alpha_+ 0.01^2 = 1 - r(1\%) \tag{6}$$

and obtain $\alpha_+ = 17$. Therefore, we investigate the parameter range between $0 \leq \alpha_+ \leq 25$ below.

It is worthwhile to rewrite Eq. 2 with the following substitutions

$$x_n = \frac{p_n - \hat{p}}{p_0 - \hat{p}} \quad , \quad C = \alpha_+ \frac{p_0}{\hat{p}} \left(\frac{p_0}{\hat{p}} - 1 \right) . \tag{7}$$

where p_0 is defined in Eq. 1. We obtain

$$x_n = 1 - C x_{n-1}^2 , \tag{8}$$

where x_n is the rescaled positron intensity; C is a stability parameter related to the gain of the feedback mechanism, to the mismatch of input scavenger intensity s_0 or $p_0 = \eta s_0$, and to the optimum positron intensity for which beam loading is compensated $\hat{p}$.

Equation 8 is the well known *logistic equation* that describes systems with a quadratic saturation mechanism, as in our model. The dynamics of Eq. 8 is very rich—depending on the parameter C, it exhibits bifurcation and even chaotic behavior. The different regimes are best represented by the Feigenbaum diagram [1] shown in Fig. 1. In the range $C < -1/4$, the dynamics are unstable; for $-1/4 < C < 3/4$, a stable, period-1 fixed point exists. Between 3/4 and 5/4, a period-2 fixed point exists, which means that the positron intensity varies on alternate pulses.

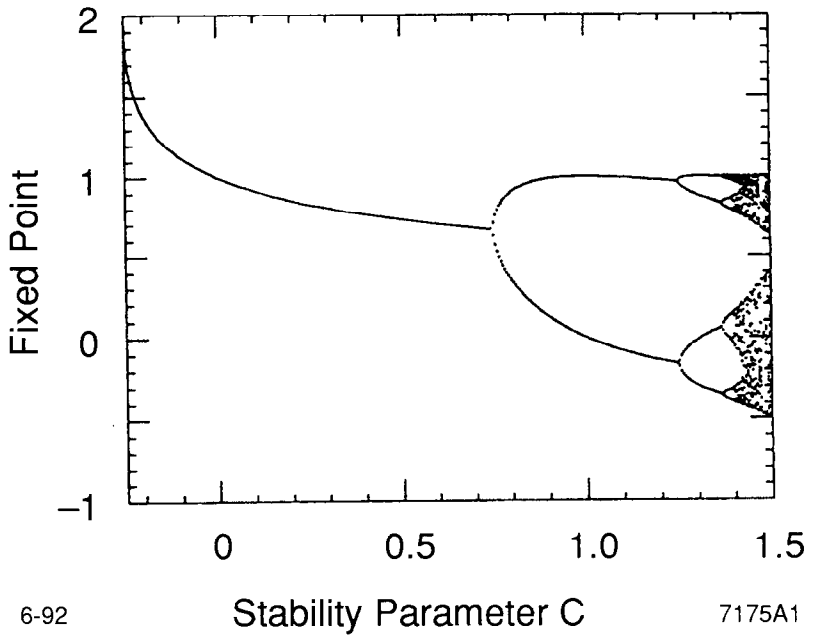

Figure 1. The fixed points of the logistic map given by Eq. 8 for parameter values of $-1/4 < C < 3/2$. *Note the sequence of bifurcations starting at* $C = 3/4$.

Between 5/4 and 1.401155189..., the system goes through an infinite series of bifurcations until it enters the chaotic regime.

The investigation of this map and its implications for the positron system is the topic of the following sections.

III. FIXED POINT

The period-1 fixed point of the iterated map given by Eq. 2 or Eq. 8 describes a special state that reproduces itself. It can be considered the equilibrium state. Whether this state is stable or unstable is addressed below. The period-1 fixed point x_∞ is defined by the equation

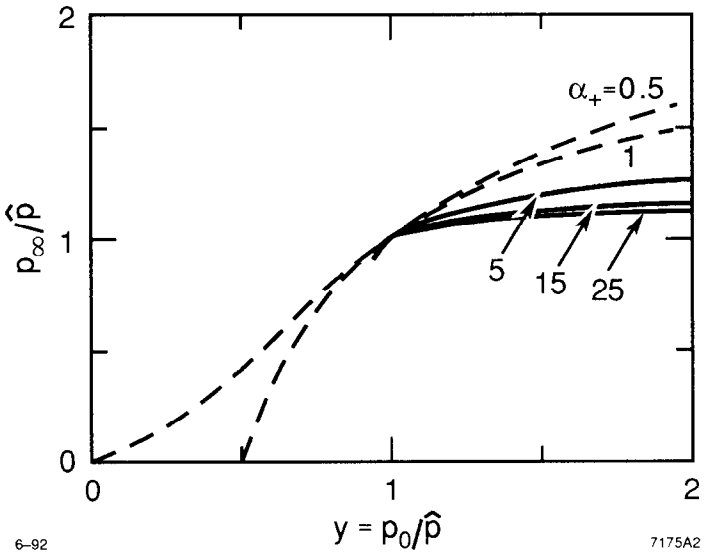

Figure 2. The normalized equilibrium positron intensity at Sector 19, $p_\infty/\hat{p}$, as a function of the normalized positron intensity without feedback mechanism $y = p_0/\hat{p}$ for $\alpha_+ = 0.5, 1$ (dashed) and $\alpha_+ = 5, 15, 25$ (solid).

$$x_\infty = 1 - Cx_\infty^2 \ , \tag{9}$$

which can be solved for x_∞ with the result

$$x_\infty = \frac{1}{2C}\left[\pm\sqrt{1+4C} - 1\right] \ . \tag{10}$$

Rewritten for the positron intensities, we get

$$\frac{p_\infty}{\hat{p}} = 1 + \frac{1}{2\alpha_+ y}\left[\sqrt{1+4\alpha_+ y(y-1)} - 1\right] \ . \tag{11}$$

where we have introduced $y = p_0/\hat{p}$ and have suppressed the negative root because it leads to negative intensities. Figure 2 shows a plot of $z = p_\infty/\hat{p}$, the normalized equilibrium intensity versus $y = p_0/\hat{p}$, the mismatch between scavenger intensity,

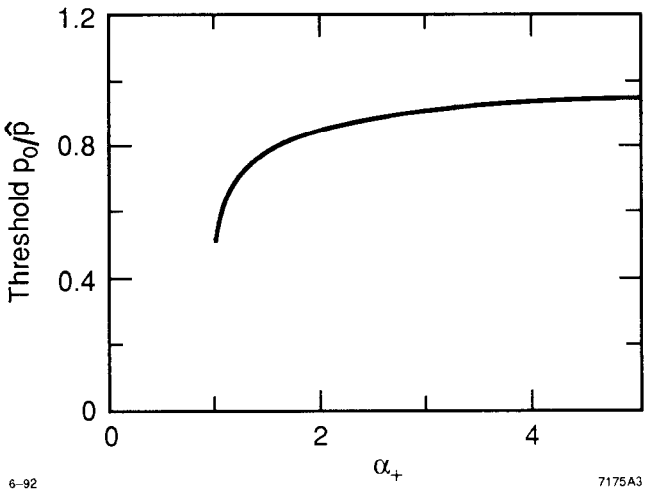

Figure 3. The threshold normalized positron intensity without feedback mechanism $y_{\rm thresh} = p_{0,\rm thresh}/\hat{p}$ *as a function of* α_+.

and beam loading compensation for different values of α_+. For $\alpha_+ \leq 1$, we always have a nonvanishing fixed-output intensity $p_\infty/\hat{p}$. However, if α_+ is increased above unity, the output intensity drops to zero if $y = p_0/\hat{p}$ falls below a threshold. This effect imposes a limit on the mismatch between the scavenger intensity s_0 and the design beam loading compensation $\hat{p}$, namely $\eta s_0/\hat{p} = p_0/\hat{p}$ may not fall below a certain value. The threshold $y_{\rm thresh} = p_{0,\rm thresh}/\hat{p}$ for a given α_+ is determined by the vanishing of the root in Eq. 11. We get

$$y_{\rm thresh} = \frac{p_{0,\rm thresh}}{\hat{p}} = \frac{1}{2}\left[1 + \sqrt{1 - 1/\alpha_+}\,\right] . \tag{12}$$

Figure 3 shows $y_{\rm thresh}$ as a function of α_+. Clearly, below $\alpha_+ = 1$, no threshold exists. For increasing α_+ the match between p_0 and $\hat{p}$ has to get increasingly better, as the threshold $y_{\rm thresh}$ gets closer to unity.

The tolerances consequently lie in the few percent range for α_+ in the range $5 \leq \alpha_+ \leq 25$. If, for a few consecutive pulses, the intensity of the scavenger bunch falls below a few percent, the positron system collapses.

A second observation is that for large α_+ (the solid lines in Fig. 2), an increased scavenger bunch intensity $y = \eta s_0/\hat{p}$ does not yield more positrons at Sector 19 as the entire system saturates, for a fixed beam loading compensation.

The previous analysis only gave a lower bound on $p_0/\hat{p}$. In the next section we perform a local stability analysis, and investigate what happens if we perturb the system around its fixed point. This analysis will also yield an upper bound.

IV. LOCAL STABILITY ANALYSIS

In order to determine whether a fixed point is stable (attractive) or unstable (repulsive), we have to perform a local, linearized stability analysis of the equation $x_n = f(x_{n-1})$. To this end, we compare the distance of the $n+1^{th}$ iteration from the fixed point x_∞ to that of the n^{th} iteration. For x_{n+1} and x_n in the vicinity of the fixed point x_∞ defined by $x_\infty = f(x_\infty)$, we write

$$\begin{aligned} x_{n+1} - x_\infty &= f(x_n - x_\infty + x_\infty) - x_\infty \\ &\approx f(x_\infty) + \frac{\partial f}{\partial x}\Big|_{x=x_\infty}(x_n - x_\infty) - x_\infty \\ &= \frac{\partial f}{\partial x}\Big|_{x=x_\infty}(x_n - x_\infty)\ . \end{aligned} \tag{13}$$

If the absolute value of the derivative of the map has an absolute value of less than unity, the fixed point is stable, because the absolute value of the distance to the fixed point decreases monotonously. From the logistic equation, Eq. 8,

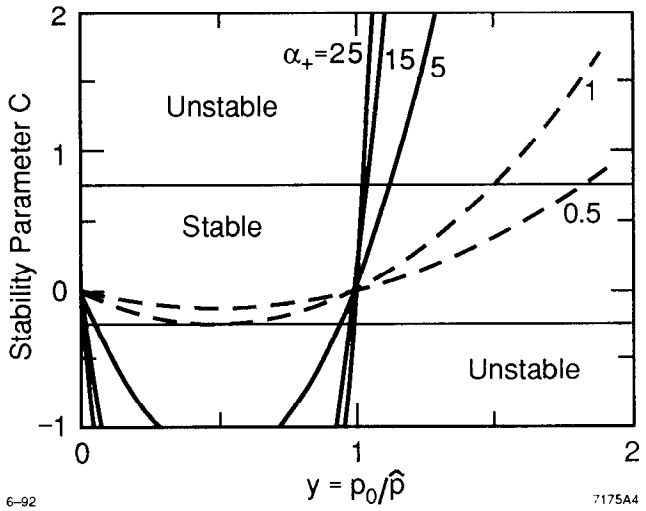

Figure 4. The stability parameter $C = \alpha_+(p_0/\hat{p})(p_0/\hat{p} - 1)$ *as a function of* $y = p_0/\hat{p}$ *for* $\alpha_+ = 0.5, 1$ *(dashed) and* $\alpha_+ = 5, 15, 25$ *(solid). For increasing* α_+ *the curves get increasingly steeper. The horizontal lines denote the stability limits according to Eq. 14.*

we obtain $f'(x) = -2Cx$. Using the value for the fixed point x_∞ from Eq. 10, we obtain $-1/4 \leq C \leq 3/4$, or

$$-\frac{1}{4} \leq \alpha_+ \frac{p_0}{\hat{p}} \left(\frac{p_0}{\hat{p}} - 1 \right) \leq \frac{3}{4} \; . \tag{14}$$

This equation constitutes the stability criterion for the fixed point. Figure 4 shows the stability parameter $C = \alpha_+(p_0/\hat{p})(p_0/\hat{p}-1)$ for various α_+ and the threshold values $C = -1/4$ and $C = 3/4$. Clearly, the bigger α_+ gets, the smaller the range of permissible mismatch between scavenger intensity and beam loading compensation gets. The limits on $p_0/\hat{p}$ at the stability threshold, we can calculate from Eq. 14 and obtain for $\alpha_+ \geq 1$

$$\frac{1}{2}\left[1+\sqrt{1-1/\alpha_+}\right] \leq \frac{p_0}{\hat{p}} \leq \frac{1}{2}\left[1+\sqrt{1+3/\alpha_+}\right] . \qquad (15)$$

and no limit for $\alpha_+ \leq 1$. The lower limit is the same as we have already encountered in Eq. 12. If the fixed point exists, it is stable. The limits given by Eq. 15 are shown in Fig. 5 as a function of α_+.

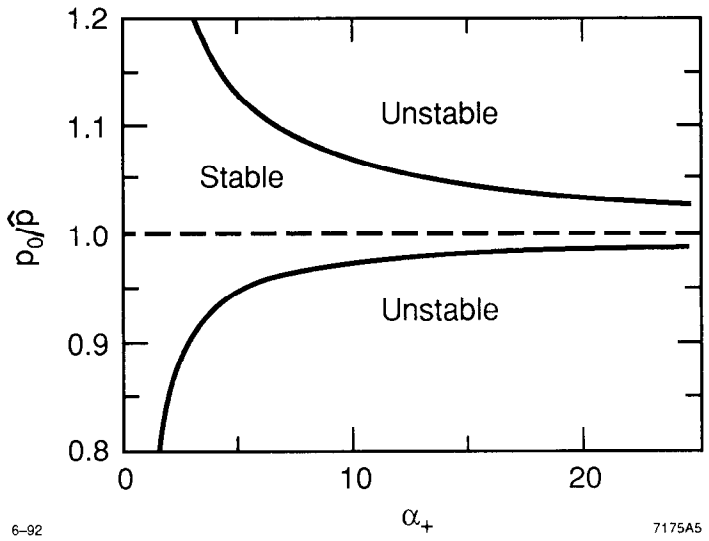

Figure 5. The stability limits as given by Eq. 15 as a function of α_+.

The upper threshold marks the point where the period-1 fixed point becomes unstable and a period-2 fixed point emerges [1,2]. This marks the first bifurcation above which the positron intensity alternates between two different values on consecutive pulses. This behavior is caused by an inherent instability of the dynamical system, and is **not** externally driven.

Again the tolerances lie in the few percent range, and get tighter as α_+ increases. However, the lower margin is tighter than the upper margin and makes a lowering of $\hat{p}$ (adjusting for lower beam loading) advisable.

V. GLITCH TOLERANCES

In this section we investigate the effect of a glitch in the scavenger bunch intensity. To do so we assume that the scavenger intensity $p_0 = \eta s_0$ was constant for a long time, such that the system has acquired its equilibrium. Then, for a single pulse, the scavenger intensity drops or increases to a new value $\tilde{p}_0$, and then resumes with p_0. By the "glitch tolerance" we mean the maximum relative deviation $\tilde{p}_0/p_0$, for which the system can recover and iterate back towards the original fixed point.

In the original stable condition, the fixed point is given by Eq. 11. If the scavenger bunch intensity assumes its new value $\tilde{p}_0$, the following positron bunch has the intensity

$$p_1 = \tilde{p}_0 \left[1 - \alpha_+ \left(\frac{p_\infty - \hat{p}}{\hat{p}} \right)^2 \right] = p_\infty \frac{\tilde{p}_0}{p_0} \,. \tag{16}$$

Then, on the next pulse the system gets back to normal, just the positron intensity is different from its equilibrium value. The original question can now be restated: how big may p_1 get and still iterate back to the fixed point? In the appendix, it is shown that for the logistic map we have to require

$$-\frac{\sqrt{1+4C}+1}{2C} < x < \frac{\sqrt{1+4C}+1}{2C} \tag{17}$$

in order for x to iterate back. Translating p_1 into x by writing $x = (p_1 - \hat{p})/(p_0 - \hat{p}) = (p_\infty \tilde{p}_0/p_0 - \hat{p})/(p_0 - \hat{p})$, we can rewrite Eq. 17 in an equation for the relative stability of $\tilde{p}_0/p_0$

$$\frac{1 - \left[\sqrt{1+4\alpha_+ y(y-1)}+1\right]/2\alpha_+ y}{1 + \left[\sqrt{1+4\alpha_+ y(y-1)}-1\right]/2\alpha_+ y} < \frac{\tilde{p}_0}{p_0} < \frac{1 + \left[\sqrt{1+4\alpha_+ y(y-1)}+1\right]/2\alpha_+ y}{1 + \left[\sqrt{1+4\alpha_+ y(y-1)}-1\right]/2\alpha_+ y} \,. \tag{18}$$

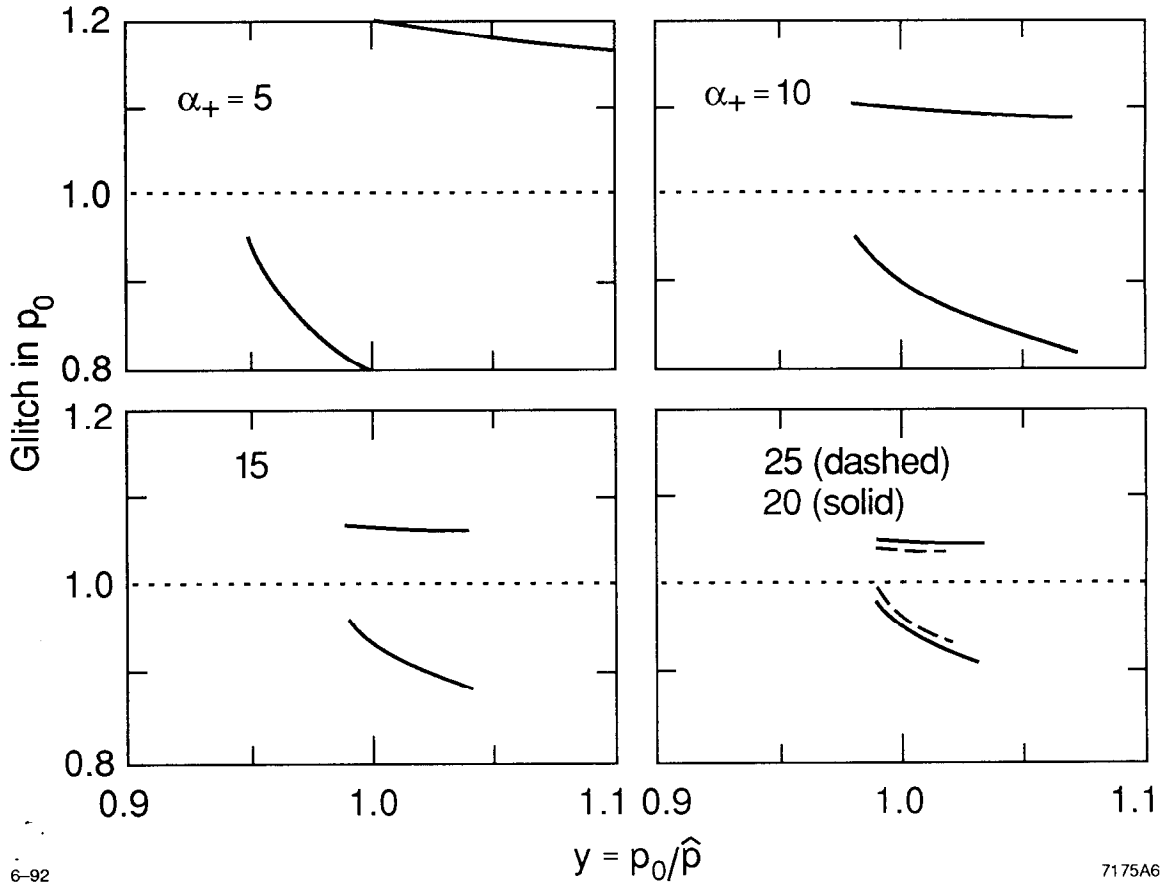

Figure 6. The permissible normalized scavenger intensity glitch amplitude $\tilde{p}_0/p_0$ as a function $p_0/\hat{p}$ for $\alpha_+ = 5, 10, 15, 20, 25$. The lines denote bounds on the permissible glitch amplitude for a given $p_0/\hat{p}$ and α_+ as described by Eq. 18.

Using Eq. 18 we can calculate the glitch tolerances for any $y = p_0/\hat{p}$ and α_+. Some examples are shown in Fig. 6. It is particularly interesting to set $y = 1$, because that defines a configuration in which the beam loading compensation ($\hat{p}$) is matched to the scavenger intensity (p_0). For this case Eq. 18 reduces to

$$1 - \frac{1}{\alpha_+} < \frac{\tilde{p}_0}{p_0} < 1 + \frac{1}{\alpha_+} \qquad \text{for } y = \frac{p_0}{\hat{p}} = 1 \ . \tag{19}$$

Consequently the tolerance with respect to single glitches is on the order of $1/\alpha_+$.

Figure 6 shows the permissible glitch amplitude as a function of $y = p_0/\hat{p}$ for various values of α_+ as the area between the solid curves. The curves only have a finite length in y, because for a given α_+ stable fixed points only exist for $y = p_0/\hat{p}$ given by Eq. 15. For increasing α_+ the permissible range becomes smaller. However, values of y slightly bigger than 1 are favorable, because there the range of permissible glitches to smaller values $\tilde{p}_0$ is bigger.

VI. JITTER TOLERANCES

We now investigate the effect of random gaussian intensity fluctuations in the scavenger intensity, parametrized by δ in $p_0(1 + \delta\hat{P})$, where $\hat{P}$ is a gaussian noise source with zero mean and unit variance. The introduction of the noise term modifies Eq. 2 to

$$p_n = p_0(1 + \delta\hat{P}) \left[1 - \alpha_+ \left(\frac{p_{n-1} - \hat{p}}{\hat{p}} \right)^2 \right] . \tag{20}$$

We then iterate this equation with the start value $p/\hat{p} = 1.001$ for a matched configuration ($p_0 = \hat{p}$) for 100 000 iterations, and check whether the motion remains stable. The jitter magnitude δ_{max} for which for a given α_+ the motion barely stays stable is plotted in Fig. 7. We see that the curve can be nicely fitted by a hyperbola of the form $0.17/\alpha_+$. Therefore, we can write for the (approximate) limit in the gaussian injection jitter

$$\delta < \delta_{max} = \frac{1}{6\alpha_+} . \tag{21}$$

We conclude that the jitter tolerance is about six times tighter than the tolerance against single glitches. For values of α_+ around ten, the jitter tolerance is on the order of 1 to 2%.

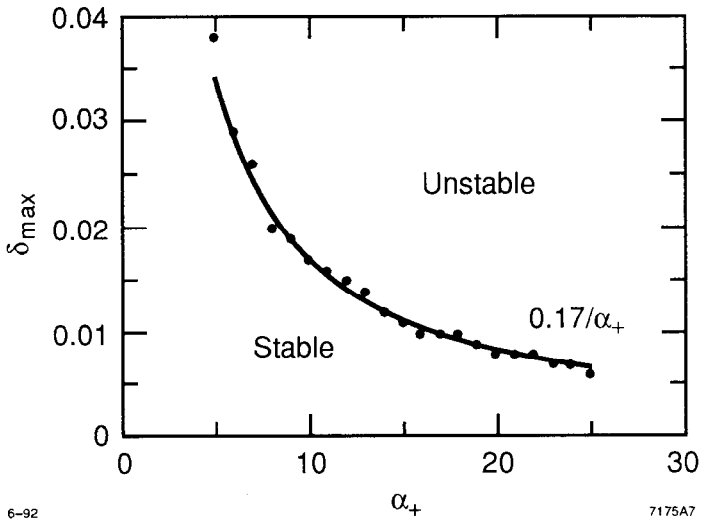

Figure 7. The maximum permissible gaussian jitter amplitude $\delta_{\max}$ *as a function of* α_+ *that survived 100 000 iterations of Eq. 20 with* $p_0 = \hat{p}$.

VII. CONCLUSION

A simple model for the positron system of the SLC was constructed, and it was shown that this model can be described by the logistic equation. Limits for the stable operation with respect to variations of the incoming scavenger bunch intensity were deduced. Variations on different time scales were investigated.

It could be shown that a permanent mismatch between the scavenger bunch intensity p_0 and the intensity for which beam loading is adjusted using linac klystron phases has to be within a few percent. The proper value depends on the value of the nonlinear "feedback" parameter α_+ and is shown in Fig. 5.

The tolerance with respect to single glitches in the scavenger intensity was shown to be considerably larger, namely in the 10% range. as shown in Fig. 6.

The system is particularly susceptible to a permanent scavenger intensity jitter, which has to be controlled to the 1 to 2% level.

All effects depend crucially on the "feedback" parameter α_+. Increasing the energy acceptance of the extraction line, and thereby lowering α_+, has improved the situation.

The model certainly can be expanded in many ways. One important aspect is the appearance of interleaved generations at 120 Hz running. In this case, two bunches are stored in the positron's damping ring, and the scavenger bunch experiences the beam loading from the positron bunch two pulses earlier. Via the possible interaction of two bunches in the damping ring, the generations can couple. Another important aspect is the inclusion of the other electron bunch, which was neglected so far. Furthermore, the recent installation of a feed-forward mechanism [3] that measures the currents of all bunches in the damping rings and adjusts linac klystron phases, in order to compensate for the scavenger energy jitter in the extraction line, couples all bunches and makes the interaction much more convoluted. On the other hand, feed-forward alleviates the problems described in this report significantly.

VIII. REFERENCES

1. G. Eilenberger, H. Müller-Krumbhaar, eds., *Ferienkurs '83. Nichtlineare Dynamik in kondensierter Materie*, Kernforschungsanlage Jülich, unpublished, 1983.

2. H. Peitgen, P. Richter, *The Beauty of Fractals*, Springer, NY, 1986.

3. R. K. Jobe, et al., *Energy Feed Forward at the SLC*, Proc. IEEE Particle Accelerator Conf., San Francisco, May 1992, pp. 1464–1466.

IX. APPENDIX: GLOBAL STABILITY OF THE PERIOD-1 FIXED POINT

In this appendix, we investigate how big the basin of attraction of the stable period-1 fixed point of the logistic map is; in other words, how far away from the fixed point we may start and still iterate towards it. To answer this question, we attempt a global stability analysis (as opposed to the local analysis of the previous section), and again consider the distance to the fixed point

$$\begin{aligned} x_{n+1} - x_\infty &= f(x_n) - f(x_\infty) \\ &= (1 - Cx_n^2) - (1 - Cx_\infty^2) \\ &= -C(x_\infty + x_n)(x_n - x_\infty) \ . \end{aligned} \tag{22}$$

The fixed point is globally stable for those points x that fulfil $|C(x_\infty + x_n)| < 1$, because then the distance will always get smaller. Inserting x_∞ from Eq. 10, we obtain

$$-\frac{\sqrt{1+4C}+1}{2C} < x < \frac{-\sqrt{1+4C}+3}{2C} \ . \tag{23}$$

This border is the only one that leads to a purely contracting mapping towards the fixed point. However, starting values of x bigger than the upper bound given by Eq. 23 can be found to iterate towards the fixed point. These additional starting points have the feature that they jump on their first iteration into the interval given by Eq. 23. Consequently, these points x have to fulfil

$$-\frac{\sqrt{1+4C}+1}{2C} < 1 - Cx^2 < \frac{-\sqrt{1+4C}+3}{2C} \ . \tag{24}$$

Solving for x leads to the following set of inequalities

$$\sqrt{\frac{-3+2C+\sqrt{1+4C}}{2C^2}} < x < \sqrt{\frac{1+2C+\sqrt{1+4C}}{2C^2}} = \frac{\sqrt{1+4C}+1}{2C} . \tag{25}$$

Since the lower bound in Eq. 25 is lower than the upper bound in Eq. 23 a sufficient condition for global stability is given by the bigger values of the borders of Eqs. 23 and 25, which are the lower bound for Eq. 23 and the upper bound for Eq. 25.

$$-\frac{\sqrt{1+4C}+1}{2C} < x < \frac{\sqrt{1+4C}+1}{2C} \tag{26}$$